Food Chemistry 320 (2020) 126639

Contents lists available at ScienceDirect

Food Chemistry

journal homepage: www.elsevier.com/locate/foodchem

Quantification of calcium in infant formula using laser-induced breakdown spectroscopy (LIBS), Fourier transform mid-infrared (FT-IR) and Raman spectroscopy combined with chemometrics including data fusion

Ming Zhao[a,e,*], Maria Markiewicz-Keszycka[b], Renwick J. Beattie[d], Maria P. Casado-Gavalda[b], Xavier Cama-Moncunill[b], Colm P. O'Donnell[a], Patrick J. Cullen[c], Carl Sullivan[b]

[a] School of Biosystems and Food Engineering, University College Dublin, Belfield, Dublin 4, Ireland
[b] School of Food Science and Environmental Health, Technological University Dublin, Cathal Brugha St, Dublin 1, Ireland
[c] School of Chemical and Bimolecular, University of Sydney, Australia
[d] J Renwick Beattie Consulting, Causeway Enterprise Agency, Ballycastle, UK
[e] The Department of Food Chemistry and Technology, Teagasc Food Research Centre, Ashtown, Dublin 15, Ireland

ARTICLE INFO

Keywords:
Laser-induced breakdown spectroscopy
Fourier transform mid-infrared
Raman spectroscopy
Chemometrics
Calcium
Infant formula

ABSTRACT

Laser-induced breakdown spectroscopy (LIBS), Fourier transform mid-infrared (FT-IR) and Raman spectroscopy combined with chemometrics were investigated to quantify calcium (Ca) content in infant formula powder (INF). INF samples (n = 51) with calcium content levels (ca. 6.5–30 mg Ca/100 kJ) were prepared in accordance with the guidelines of Commission Directive 2006/125/EC. Atomic absorption spectroscopy (AAS) was used as the reference method for Ca content determination. To predict Ca content in INF samples, partial least squares regression (PLSR) models that developed based on LIBS, Raman and FT-IR spectral data, respectively. The model developed using LIBS data achieved the best performance for the quantification of Ca content in INF (R^2 (cross-validation (CV))-0.99, RMSECV-0.29 mg/g; R^2 (prediction (P))-1, RMSEP-0.63 mg/g). PLSR models that developed based on data fusion of Raman and FT-IR spectral features obtained the second best performance (R^2CV-0.97, RMSECV-0.38 mg/g; R^2P-0.97, RMSEP-0.36 mg/g). This study demonstrated the potential of LIBS, FT-IR and Raman spectroscopy to accurately quantify Ca content in INF.

1. Introduction

Breastfeeding provides optimal nutrition to human infants (Harding, Cormack, Alexander, Alsweiler, & Bloomfield, 2017). However, most infants worldwide are not breastfed according to a WHO funded study on feeding practices of infants and young children (Victora et al., 2016). Infant formula (INF) is the only appropriate substitute for breast milk. It provides all essential nutrients to support adequate growth and development of infants and young children (Rollins et al., 2016). When INF is a sole source of nutrients for neonates, optimal mineral compositions of INF become critical to sustain human body growth and development.

Dairy-based INF is usually made from bovine skim milk, which must be modified to suit the needs of neonates (Ahmad & Guo, 2014). Calcium is one of the most important micronutrients contained in milk. It is required for normal growth and the development of the skeleton and teeth of mammals (Arifin, Swedlund, Hemar, & McKinnon, 2014). Calcium in INF always occurs in the form of salts or is associated with other dietary constituents in the form of complexes of calcium ions (Strain & Cashman, 2002). Ca content in INF can be modified by the addition of lactose and demineralised whey powder to dilute Ca; and by the addition of calcium salts (e.g. $CaCO_3$) and other INF premixes to enhance Ca content (Smith, Gordon, & Holroyd, 2013). Infant formula production involves several processing steps and varies between manufacturers (Ahmad & Guo, 2014). According to the report of Euromonitor International, global sales of baby milk formula could be worth USD 71 billion in 2019 (Rollins et al., 2016). Hence, the dairy industry is expecting the development of low-cost process analytical technologies (PAT) with the real-time monitoring capabilities to assure consistent quality control (Cullen, O'Donnell, & Fagan, 2014).

Two principal techniques for detection and determination of minerals in INF are atomic absorption spectroscopy (AAS) and inductively coupled plasma optical emission spectrometry/mass spectrometry (ICP-OES/MS) (Walsh, 2014). These techniques are capable to determine

* Corresponding author.
E-mail addresses: ming.zhao@ucd.ie, ming.zhao@teagasc.ie (M. Zhao).

https://doi.org/10.1016/j.foodchem.2020.126639
Received 22 November 2019; Received in revised form 29 February 2020; Accepted 17 March 2020
Available online 19 March 2020
0308-8146/

elements at ultra-trace levels but only suitable for laboratory use. Sophisticated instrumentation and time-consuming sample digestion procedures are in demand; therefore, these techniques cannot meet the requirements for real-time measurements.

Laser-induced breakdown spectroscopy (LIBS) is an atomic emission spectroscopic technique which uses focused pulsed laser beam to generate plasma from the analytic material. A small amount of material is ablated, producing a plasma plume which consists of atoms, ions and free electrons. As the plasma cools down, the atoms, ions and electrons lose energy and emit light with specific spectral characteristics for each element existing in the target material (Markiewicz-Keszycka et al., 2018). LIBS has been reported to quantify Ca in INF (Cama-Moncunill et al., 2017) with a R^2CV value of 0.90 and a RMSECV value of 0.62 mg/g.

Both of mid-infrared (MIR) and Raman are spectroscopic techniques involving vibrational transitions. In MIR spectroscopy, the transitions between energy levels of a molecule are induced by the absorption of infrared radiation. An 'infrared-active' molecule must show an electric dipole moment which is changed by vibration. The dipole moment of such a molecule changes as the chemical bond expands and contracts when absorbing and emitting infrared light; in Raman spectroscopy, vibrational transitions occur during the scattering of light by molecules. Molecular vibrations can be described as motions of atoms in a molecule. All the atoms vibrate at a certain characteristic frequency. While MIR requires a change in dipole moment during vibration, which usually requires some polarity difference between the ends of chemical bonds, Raman technique requires a polarisable change, which is ease of introducing a polarity. Moreover, MIR spectroscopy is more active to polar bonds (in asymmetric stretch mode) while Raman spectroscopy is more active to non-polar bonds (in symmetric stretch mode). Other chemical bonds somewhere in between may be weakly allowed in both techniques (Bunaciu & Aboul-Enein, 2017; Socrates, 2002). MIR for the prediction of major minerals including calcium in milk with moderate accuracy (R^2CVs-0.58–0.68, RMSECVs-120–153.02 mg/kg) (Visentin, Penasa, Gottardo, Cassandro, & De Marchi, 2016) and poor accuracy (R^2CV-0.48; RMSECV-131 mg/L)) (Bonfatti, Degano, Menegoz, & Carnier, 2016). Fourier transform mid-infrared (FT-IR) technique has been introduced to eliminate biases which are associated with the standard infrared methods in order to enhance infrared spectral features (Juanéda, Ledoux, & Sébédio, 2007). Raman spectroscopy is excellent for the detection of multi-nuclear ions that contain polarisable bonds, including phosphates, carbonates, etc. Calcium mainly exists as calcium phosphate and $CaCO_3$ in a milk based infant formula (Smith et al., 2013). Very few publications have reported the use of Raman spectroscopy to detect mineral content in dairy products. Smith et al. reported using Fourier-transform Raman spectroscopy to detect and quantify calcite in milk powder (Smith et al., 2013). However, both MIR and Raman spectroscopic techniques are not adopted for the direct detection and determination of minerals; it is due to the absence of sufficient fundamental studies in this area. While on the other hand, it has demonstrated that a correlation exists between the numbers of cations and that of their corresponding anions in a neutral chemical complex (Chukanov, 2014). Some previous studies have reported the customary application of Raman spectroscopy or middle infrared for the investigation of minerals by the identification of different groups of atoms using spectral wavelength bands (Chou & Wang, 2017; Chukanov, 2014). Recently, Raman spectroscopy was used to develop a rapid tool for the estimation of calcium and ash contents in bone and meat mixtures and obtained a R^2CV value of 0.775 and a RMSECV value of 0.33% for Ca content prediction (Wubshet, Wold, Böcker, Sanden, & Afseth, 2019). Therefore, Raman and MIR spectroscopy combined with multivariate data analysis hold the potential to quantify mineral cations in a chemical complex via directly determination of their corresponding anions. In addition, the combination of Raman and MIR spectral features would give complementary information for the quantification of minerals in INF.

In this study, the potential of Raman, FT-IR and LIBS were evaluated to determine calcium content in powdered infant formula. This investigation was conducted with the objective to develop a mathematical model for accurate quantification of calcium content in INF powder using LIBS, FTIR and Raman spectroscopy combined with chemometric approaches including data fusion strategies to accomplish complementary spectral information for the quantification purpose.

2. Material and methods

2.1. Sample preparation

According to the Commission Directive 2006/141/EC (European, 2006), the content of Ca in INF manufactured from cows' milk should be in a range of 12–33 mg Ca/100 kJ. Ca content in the INF mixtures used in this experiment was arranged from 6.5 to 30 mg Ca/100 kJ. Commercial INF intended for children from 0 to 6 months was purchased from local stores in Dublin, Ireland. Five calibration sample formulae (Ca1, Ca2, Ca3, Ca4, Ca5) and 2 validation sample formulae (CaV1, CaV2) were designed for the study. To obtain sample formulae (Ca1, Ca2 and CaV1) at lower Ca content levels, lactose (α-lactose monohydrate ≥99%) was added into the purchased commercial INF powder (Ca3). In order to obtain homogenous samples with higher amount of Ca, a premix sample (Premix1) containing 99 mg Ca/100 kJ was prepared by blending 96 g of INF with 4 g of calcium carbonate ($CaCO_3$ ≥99%); Premix1 was subsequently diluted using INF (Ca3) to get another premix sample (Premix2) with Ca content of 48 mg Ca/100 kJ. Premix2 was used as Ca source for preparation of other sample formulae (Ca4, CaV2 and Ca5). Each blend was prepared in the amount of 100 g. The details of sample formulation are shown in Supplementary (I).

To ensure accurate mixing of INF with $CaCO_3$ and lactose, the blending process was divided into two parts. Firstly, to reduce and homogenise particle size, mixtures were ground in a laboratory blender (8011G, Waring Laboratory Science, CT, USA) equipped with rotatory stainless-steel blades for 2 min. Then the blends were transferred into a laboratory V-mixer (FTLMV-1L&, Filtra Vibration S.L., Spain) and the dry mixing was applied for 20 min. Sample powder was then pelleted using a hydraulic press (GS01160, Specac Ltd., Orpington, U.K.) by applying a pressure of 10 tonnes for 3 min. Samples were prepared in triplicate for three batches following each calibration sample formula, the five formulae (i.e. Ca1, Ca2, Ca3, Ca4 and Ca5) were followed; therefore, 45 pellet samples were obtained for the calibration group. Six pellet samples were also prepared by following the two formulae (i.e. CaV1 and CaV2) of the validation group for three times. In total, 51 sample were prepared for this study. All chemicals used in the experiments presented in this paper were purchased from Sigma Aldrich (Arklow, Ireland).

2.2. Atomic absorption spectroscopy analysis

Calcium content in all samples were determined using atomic absorption spectroscopy (AAS) (Varian 55B AA, Agilent Technologies, United States). Sample digestion was conducted in MarsXpress® vessels in a microwave accelerated reaction system (CEM Corp. MARS 6, Matthews, NC, USA) following the CEM digestion procedure for powdered infant formula. In brief, 500 mg of each sample was weighed in the MarsXpress® vessels and then 10.0 mL of 69% HNO_3 (CAS 7697-37-2, Sigma Aldrich, Inc.) was added. The microwave heating program consisted of ramping from the ambient temperature to 200 °C in 20 min and holding this temperature for 15 min. After cooling, the residual solution of each sample was transferred into a 50 mL volumetric flask and the volume was made up with high-purity deionized water. Further dilutions using deionized water were carried out to maintain Ca concentrations within the AAS optimum measurement range (0–3 ppm). An air-acetylene type flame was used for AAS analysis. To avoid

interferences in air-acetylene, calcium content was determined in the presence of lanthanum chloride solution. The metal-specific hallow cathode lamp with an operating electrical current of 4 mA was used as the radiation source. Ca absorbance was measured at the wavelength of 422.7 nm with a slit width of 0.5 nm. Calibration curves were established by using aqueous standards prepared from a commercial calcium stock solution (Calcium standard for AAS – 1000 mg L^{-1}, Sigma-Aldrich).

2.3. LIBS

The spectra of LIBS were obtained by using a LIBSCAN-150 system (Applied Photonics, UK) and six fibre-optic compact optical spectrometers (Avantes, AvaSpec, Netherlands), which covered the spectral range of 181.4–904.2 nm. The laser was operated in Q-switched mode at a repetition rate of 2 Hz and 100 mJ/pulse, whereas the spectrometer was operated at 1.27 μs gate delay and 1.1 ms integration time. Each pellet was analysed at 100 different locations, directly in the air using a controlled X-Y-Z translation stage (XYZ- 750, Applied Photonics Limited, Skipton North Yorkshire, United Kingdom). To obtain the best signal-to-noise ratio, each spectrum was acquired as the result of two accumulations for each location. The spectra were obtained at a constant optimum focal length of 76 mm.

2.4. Raman spectroscopy

Raman spectra were collected using DXR SmartRaman spectrometer (ThermoFisher Scientific UK Ltd., Loughborough, UK) equipped with a diode laser operating at 780 nm to minimise sample fluorescence issues and a charge coupled device (CCD) detector. One side of the sample pellet was placed over the aperture (50 μm slit) on the 180-degree platform sampling accessory. All spectra of each sample were accumulated for 5 min (i.e. 15 s exposure time × 20 exposures) using a 150-mW laser power. Samples were scanned in a random order at ambient temperature (ca. 20 °C). Raman intensity counts per second (cps) were recorded over the wavelength range 250–3380 cm^{-1} at 2 cm^{-1} intervals. Cosmic spikes were removed automatically by the supplied software. Instrument control, spectral acquisition and file conversion were performed using the supplied OMNIC software v 9.2.98 (Thermo Fisher Scientific Inc., USA). Each sample was scanned twice at two different locations on the sample pellet; the mean of these duplicate spectra was used in subsequent chemometric operations.

2.5. FT-IR spectroscopy

The spectra of the samples were collected using Nicolet™ iS5 (Thermo Scientific, USA) Fourier transform mid-infrared spectrometer equipped with diamond crystal attenuated total reflectance (ATR) accessory (iD7 ATR, Thermo Scientific, USA). For analysis, one side of the sample pellet was placed on the ATR crystal to cover the entire crystal surface. Single beam reflectance spectra were recorded over the wavenumber range 250–4000 cm^{-1} with a resolution of 2 cm^{-1}. Background calibration was carried out using air blank reference before each measurement. Cleaning procedures were carried out before and after each measurement using ethanol (99%) to wipe the ATR crystal. During each measurement, 64 scans were performed and averaged. Spectral data were recorded using the supplied OMNIC software v 9.2.98 (Thermo Fisher Scientific Inc., USA). Each sample was measured in triplicate and the mean value was acquired for chemometric analysis.

2.6. Chemometric analysis and data fusion

Both raw Raman and FT-IR spectra were exported from OMNIC software as .csv files and imported into Matlab 2018a (The Mathworks, Natick, MA, USA). LIBS spectral data were imported into R (The R Foundation for Statistical Computing, Austria). The mean spectrum of each sample was calculated; baseline correction on raw data was carried out using asymmetric least squares correction (AsLs).

Basic statistics on the analysis (including mean and standard deviations) of AAS were summarized. The mean Ca content value of each sample was used as the chemical reference (Y-variables); the collected full spectral variables or variables in the selected wavelength ranges of each spectroscopic technique were used as X-variables for the development of partial least squares regression (PLSR) models. The optimal wavelength ranges used in modelling were selected on the basis of observed spectral signal intensities. PLSR models were developed using the nonlinear iterative partial least squares (NIPALS) algorithm on the calibration samples (n = 45) and validated using independent validation samples (n = 6). Leave-one-out cross-validation was carried out. To evaluate model performance, parameters such as root mean square error of cross-validation (RMSECV) and prediction (RMSEP) as well as regression coefficients of determination on cross-validation (R^2CV) and prediction (R^2P) were calculated. The bias of cross-validation and prediction was also determined. Robustness of PLSR models were enhanced using the most relevant spectral variables which were selected by variable importance on projection (VIP) (Chong & Jun, 2005).

To achieve more accurate prediction results, PLSR models were also developed based on complementary information of both Raman and FT-IR spectral variables and features. Two data fusion strategies were studied and compared (Fig. 1). The first approach was based on the lower level fusion of both Raman and FT-IR spectral data in the same selected wavelength range (450–2800 cm^{-1}). The selected Raman and FT-IR spectral variables were fused into one data frame by concatenation (Fig. 1- Data fusion(I)A) or by coaddition (Fig. 1-Data fusion(I)B). The second approach was based on the mid-level fusion of scores corresponding to the optimal latent variables used for the PLSR modelling also based on Raman and FT-IR spectral data (450–2800 cm^{-1}) (Fig. 1-Data fusion(II)). VIP variable selection algorithm was used to assist the selection of the most relevant spectral variables for Ca content prediction in the lower fusion level. VIP is also a necessary procedure carried out before the PLS modelling that generate optimal latent variables used for the mid-level fusion of their relevant scores.

The limit of detection (LOD) values of the best performed PLSR models were also calculated. LOD is the smallest amount or concentration of an analyte in the test sample that can be reliably distinguished. Pseudo-univariate LOD (LOD_{pu}) takes into account the uncertainty of the calibration line and considers α and β probabilities of error. The international union of pure and applied chemistry (IUPAC) recommended LOD formula as below:

$$LOD_{pu} = 3.3 s_{pu}^{-1} [(1 + h_{0min} + 1/I) var_{pu}]^{\frac{1}{2}}$$

where s_{pu}^{-1} is the slope of the pseudo-univariate line, h_{0min} is the minimum leverage when the concentration of analyte is 0, I is the number of samples, var_{pu} is the variance of the regression residuals (Allegrini & Olivieri, 2014).

3. Results and discussion

3.1. Results and discussion of experiments

3.1.1. AAS results of Ca content

Atomic absorption spectroscopy (AAS) was performed as a reference method to determine Ca content in all samples. The accuracy of AAS results depends on the calibration curve obtained using standard solutions of the examined element. The calibration curve obtained in the current study exhibited linearity with a coefficient of determination (R^2) of 0.97. The statistics of AAS analysis was summarized in Table 1. Mean values and the low standard deviation values (i.e. 0.01–0.23 mg/g) were derived based on the AAS results of samples that prepared following each formula. As samples were prepared following each formula in three batches; the mean value of the measured Ca content

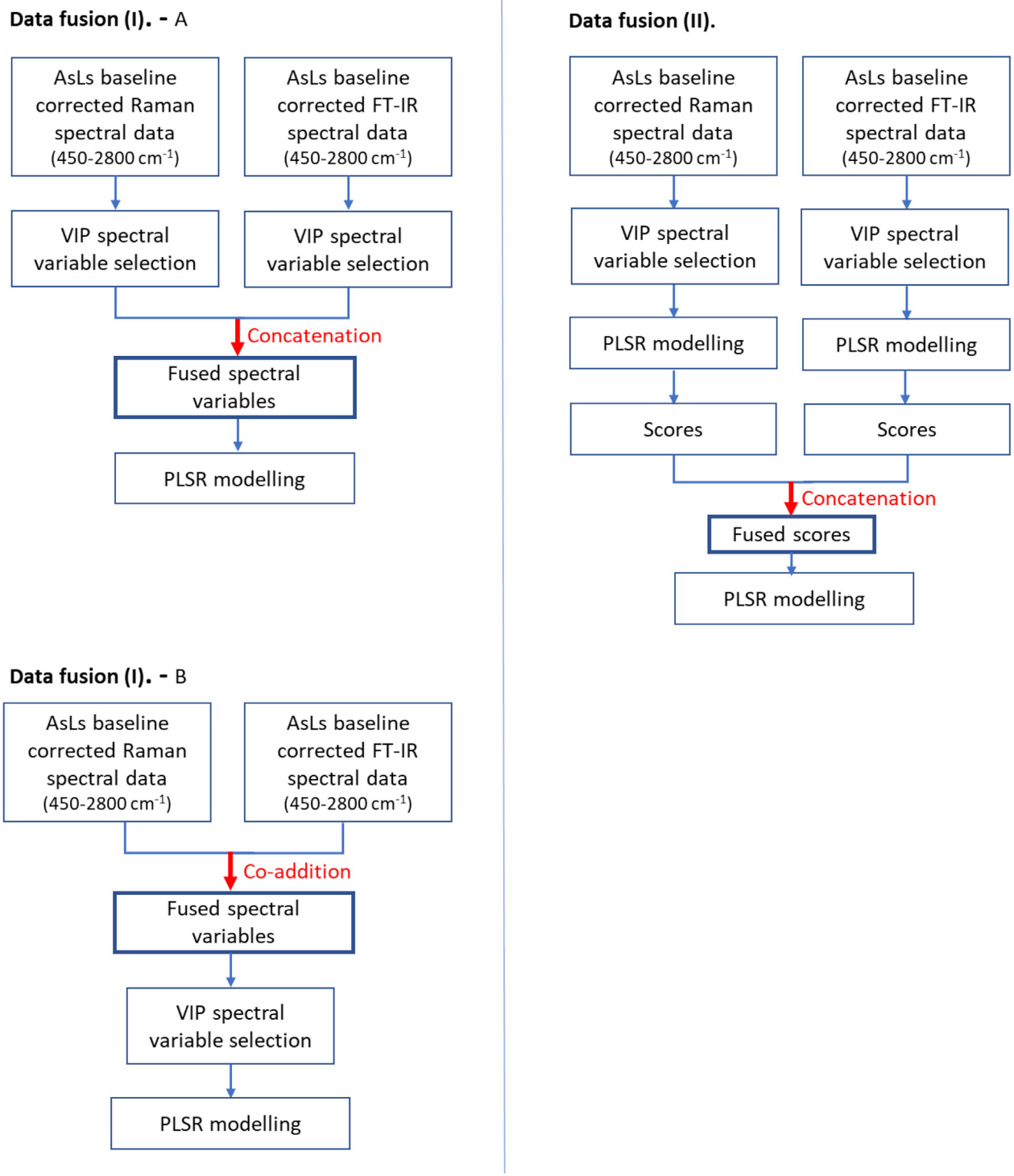

Fig. 1. The illustration of data fusion strategies.

showed no significant -differences ($P > 0.05$) between batches, while the visible variations -were possibly caused by some sample handling procedures and the dry mixing process. However, the measured Ca content levels (ca. 1.08–8.33 mg/g) of samples prepared in three batches are around the estimated Ca content levels (ca. 1–6.17 mg/g) in Supplementary (I). Nevertheless, the Ca contents determined by AAS are generally higher than the estimated values that based on calcium contents provided by the INF manufacturer.

3.1.2. LIBS spectra

For each sample, the LIBS spectrum was derived from the averaged value of three hundred spectra (100 scans * 3 replicates). Based on the reference NIST database, 25 emission lines related to calcium have been identified (Kramida, Ralchenko, & Reader, 2016). High intensities of Ca emission lines can be observed at 317.93, 393.36, 396.84 and 422.67 nm, while the highest intensity of LIBS wavelength (589.05 nm) is related to the emission of Na ions. The LIB spectral features (Fig. 2a) were as the same as the LIBS spectra of INF powder which have been reported in a previous publication (Cama-Moncunill et al., 2017).

Table 1
Ca content in dry matter (DM) of INF and the INF mixtures determined by AAS.

Batch	Sample type	Ca content*(mg/g DM)
Calibration 1	Ca1	1.09 ± 0.01
	Ca2	3.01 ± 0.03
	Ca3	4.49 ± 0.04
	Ca4	5.88 ± 0.05
	Ca5	7.44 ± 0.22
Calibration 2	Ca1	1.24 ± 0.11
	Ca2	3.89 ± 0.13
	Ca3	5.31 ± 0.11
	Ca4	6.69 ± 0.18
	Ca5	8.10 ± 0.23
Calibration 3	Ca1	1.31 ± 0.08
	Ca2	3.41 ± 0.18
	Ca3	5.39 ± 0.09
	Ca4	5.98 ± 0.16
	Ca5	7.73 ± 0.20
Validation	CaV1	4.31 ± 0.10
	CaV2	7.55 ± 0.17

*Mean ± standard deviation.

Fig. 2a shows the mean spectrum of samples (Ca1, Ca3 and Ca5) which contain low, medium and high levels of Ca content respectively. In Fig. 2a, the spectrum of the sample Ca5 shows higher intensities of Ca bands than the spectra of samples Ca1 and Ca3. The emission bands of other elements were also observed in the spectra including C_2, Na, H, N, K and O. Additionally, molecular emission bands of CN were identified at 385.034–385.427 nm, 386.163–388.308 nm and 416.721–419.698 nm; while the intensities of LIBS wavelengths related to CN, C, H, N and O didn't show obvious differences but showed differences on the wavelengths related to C_2. The detected organic atoms (i.e. C, H, N, O and CN) refer to the organic compounds of INF or can originate from the surrounding air.

3.1.3. Raman spectra

Raman spectral details are shown on the mean spectrum in the frequency range of 50–3398 cm^{-1} (Fig. 2b). Raman spectral bands at 357, 445, 850, 877, 950, 1064 and 1085 cm^{-1} are assigned to the vibrational mode of the glycosidic bond of α or β lactose (Kirk, Dann, Blatchford, & C., 2007; Li-Chan, 1996). Raman bands of 645, 773 and 877 cm^{-1} may relate to δ (C—C—O) or δ (C—C—H) bonds of tryptophan (Almeida, Oliveira, Stephani, & de Oliveira, 2011; Rodrigues Júnior et al., 2016); 445 and 598 cm^{-1} may relate to δ (C—C—C) and τ (C—O) bonds (Rodrigues Júnior et al., 2016); 950 cm^{-1} has been assigned to δ (C—O—C), δ (C—O—H) and ν (C—O) bonds; 1064, 1085 and 1121 cm^{-1} have also been assigned to δ (C—O—H), ν (C—O) and ν (C—C) of aspartic and glutamic acids (Almeida et al., 2011; Li-Chan, 1996). In the previous studies, Raman spectral signals around 1003 cm^{-1} were strongly related to the ring-breathing structure of phenylalanine (Almeida et al., 2011; Beattie, Bell, Farmer, Moss, & Patterson, 2004; Li-Chan, 1996; Rodrigues Júnior et al., 2016; Zhao, Beattie, Fearon, O'Donnell, & Downey, 2015). Prominent Raman peaks at 1262, 1442 and 1745 cm^{-1} are respectively assigned to γ (CH_2), τ (CH_2), δ (CH_2) and ν (C═O) bonds of aliphatic chains in lipids and amino acid residues (Beattie et al., 2004; Li-Chan, 1996; Rodrigues Júnior et al., 2016). Raman bands around 1555 and 1654 cm^{-1} are respectively related to δ (N—H) and ν (C═N) of Amide II, and ν (C═O) of Amide I (Almeida et al., 2011; Rodrigues Júnior et al., 2016). The region of 2855 and 2900 cm^{-1} may be attributed to symmetric ν (CH_2) and asymmetric ν (CH_3) modes while the region of 3005 cm^{-1} may result from the symmetric γ (CH_2) vibrational mode of aliphatic chain and aromatic structures of lipids (El-abassy, Eravuchira, Donfack, von der Kammer, & Materny, 2011).

3.1.4. FT-IR spectra

The details of the mean FT-IR spectrum are shown in the frequency

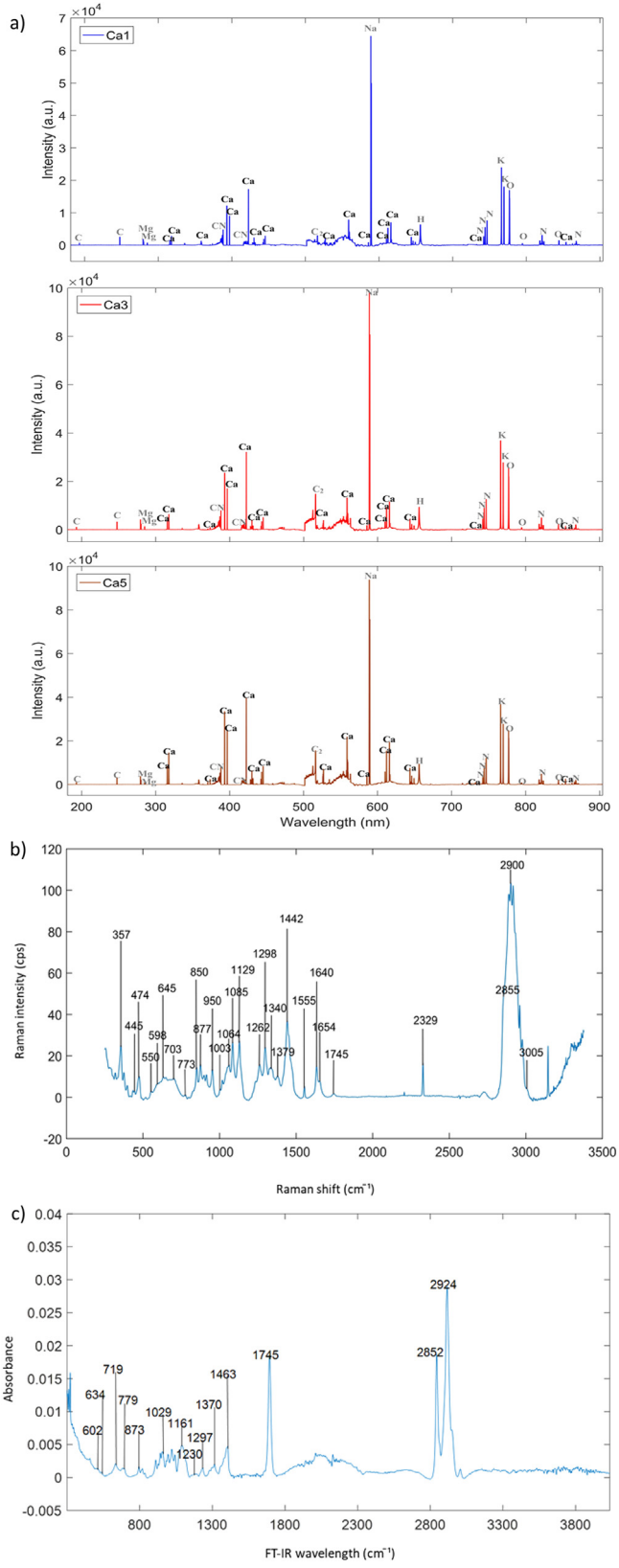

Fig. 2. a) Averaged LIBS spectrum (181–904 nm) of INF sample - Ca1, Ca3 and Ca5 with low, medium and high Ca concentration, respectively; b) averaged Raman spectrum pre-treated by AsLs baseline correction over the Raman frequency range (250–3380 cm^{-1}); c) averaged FT-IR spectrum pre-treated by AsLs baseline correction over the Raman frequency range (400–4000 cm^{-1}).

range of 400–4000 cm^{-1} (Fig. 2c). The absorption peak at 634 cm^{-1} is assigned to δ (*N*—C═O) of Amide II and III; the peak at 719 cm^{-1} is related to δ (N—H) of Amide I; peaks at 779 and 1297 cm^{-1} are related to δ (N—H) of amine salts and Amide III, respectively (Socrates, 2002). Other peaks at 1230, 1370 and 1463 cm^{-1} are related to ν (CH_2) of aliphatic chains of fatty acids (Safar, Bertrand, Robert, Devaux, Genot, 1994). Absorption bands of 873, 1409 and 1450 cm^{-1} are assigned to ν (CO_3^{2-}) (Fleet, 2017). Bands at 602 and 1029 cm^{-1} are assigned to ν (PO_4^{3-}) (Liu, Eriksson, Jin, Nygren, & Shen, 2014). Peaks at 1161 and 1745 cm^{-1} are assigned to ν (C—O) and peaks at 2852 and 2924 cm^{-1} are attributed to asymmetric ν (CH_2) and symmetric ν (CH_2) of fatty acids (Lei et al., 2010).

3.2. PLSR models developed using individual spectral data of each technique

The PLSR models were developed using the full range of LIBS (181.4–904.2 nm) including massive spectral variables (n = 11660) and the VIP selected spectral variables (n = 4516). One model was also developed using the spectral variables (n = 75) with high signal intensities related to Ca content which were provided by the NIST database as a reference. The best-performed model was developed using VIP selected spectral variables and three PLS loadings achieved a R^2CV value of 0.985 with a RMSECV value of 0.287 mg/g and a R^2P value of 0.996 with a RMSEP value of 0.634 mg/g (Fig. 3a & b).

For the prediction of Ca using Raman spectroscopy, PLSR models were developed using VIP selected spectral variables in a series of Raman frequency ranges including 250–1800, 250–3000, 450–3000, 450–2800 and 800–1800 cm^{-1} respectively and the collected full spectral range in 250–3380 cm^{-1}. Results showed that the model developed using all the collected Raman spectral variables (n = 3246) had the relatively poor performance for Ca prediction, which revealed a R^2CV value of 0.76 with a RMSECV value of 1.15 mg/g and a R^2P value of 0.61 with a RMSEP value of 1.36 mg/g. However, model prediction performance was improved significantly using VIP variable selection algorithm to eliminate the non-relevant spectral variables. Generally, four PLS loadings were required for PLSR modelling which yielded R^2CVs of 0.89–0.95 with RMSECVs of 0.49–0.75 mg/g and R^2Ps of 0.87–0.97 with RMSEPs of 0.51–0.95 mg/g. The best-performed prediction model developed using VIP selected Raman spectral variables (n = 638) in the wavelength range of 450–2800 cm^{-1} achieved a R^2CV value of 0.954 with a RMSECV value of 0.490 mg/g and a R^2P value of 0.964 with a RMSEP value of 0.532 mg/g (Fig. 3c & d).

The PLSR model developed using all the collected FT-IR spectral variables (n = 3734) had a poor performance for Ca prediction due to the interferences of the non-informative spectral variables. However, after VIP variable selection, models developed based on the retained spectral variables achieved R^2CVs of 0.71–0.85 with RMSECVs of 0.89–1.23 mg/g and R^2Ps of 0.68–0.91 with RMSEPs of 0.6–1.24 mg/g. The best-performed model (Fig. 3e & f) was developed using seven PLS loadings and VIP selected spectral variables (n = 190) in the wavelength range of 450–2800 cm^{-1} to achieve a R^2P value of 0.905 with a RMSEP value of 0.604 mg/g.

In addition, the summary of the performances of all the PLSR models developed using LIBS, Raman and FT-IR spectroscopy for the prediction of Ca content in INF was shown in a table of Supplementary (II).

3.3. PLSR models developed using Raman and FT-IR spectra using data fusion strategies

Raman and FT-IR spectroscopic techniques can be complementary to each other for the determination of the anions of the chemical compounds in INF powder. Calcium exists in INF as cations which are strongly correlated to the anions. Therefore, PLSR models developed using the combination of Raman and FT-IR spectral information would be helpful to improve the prediction accuracy on Ca. Based on the best performance of PLSR models developed using individual Raman or FT-IR spectral data, data fusion was carried out using spectral features in the same wavelength range (450–2800 cm^{-1}) of both Raman and FT-IR spectroscopy. The first strategy of data fusion-(I)-A (Fig. 1) was developed to concatenate the VIP selected spectral variables while both spectral data were pre-treated using normalisation and group scaling and consequently to reform as a new data frame (51 samples * 828 spectral variables). The regression coefficient intensities (arbitrary units (a.u.)) of the fused spectral data were derived from PLSR modelling using four latent variables (LVs); high regression coefficient intensities were related to Raman spectral variables while very low intensities were related to FT-IR spectral variables. The PLSR model developed on the strategy of data fusion-(I)-A yielded a R^2CV value of 0.933 with a RMSECV value of 0.592 mg/g and a R^2P value of 0.939 with a RMSEP value of 0.792 mg/g; as shown in Supplementary (III). The results were more accurate than that of the models developed using individual FT-IR spectral variables and slightly less accurate than those developed using the individual Raman spectral variables.

In the strategy of data fusion-(I)-B (Fig. 1), both matrices of Raman and FT-IR spectral data (450–2800 cm^{-1}) of 51 samples were co-added together to form a new data frame (51 samples*2438 spectral variables); then the PLSR model was developed using VIP selected spectral variables (n = 283) and acquiring three LVs. The results achieved by this strategy were slightly more accurate than those achieved by the previous strategy - Data fusion (I)-A with a R^2CV value of 0.950 with a RMSECV value of 0.514 mg/g and a R^2P value of 0.958 with a RMSEP value of 0.704 mg/g.

Furtherly, a middle level of data fusion was carried out using the second strategy of data fusion – data fusion (II) (Fig. 1). The aim of PLSR modelling using the VIP selected Raman or FT-IR spectral variable matrices (X) and the Ca reference array (Y) was to extract the latent variable (LV) score matrices. To extract LV score matrices, the covariance between X and Y were maximised by adding the weights of regression coefficients of the related spectral variables (as the orthogonal matrices (B)) to the scores of X. Fig. 4a and b illustrate the mechanism of the score extraction procedures. In this study, the first four LV scores of the model developed using Raman spectral data and the first seven LV scores of that developed using FT-IR spectral data were concatenated to form a new data frame (51 samples * 11 LVs), which was plotted out in Fig. 4c. For a further PLS modelling based on the new data frame, the regression coefficients related to Raman scores exhibited a higher intensity than those related to FT-IR scores (Fig. 4d). A model developed using the fused scores achieved a R^2CV value of 0.973 with a RMSECV value of 0.378 mg/g and a R^2P value of 0.968 with a RMSEP value of 0.368 mg/g; two PLS loadings were required for the model development (Fig. 4e & f).

3.4. Discussion on the performance of PLSR models developed using LIBS, FT-IR and Raman spectra

The minerals present in cows' milk-based INF occur as inorganic ions and salts or form complexes with proteins and peptides, carbohydrates, fats and small molecules (Vegarud, Langsrud, & Svenning, 2000). Ca ions chelate to milk proteins and peptides such as α_{s1}-casein, α_{s2}-casein, β-casein, γ-casein, whey proteins, β-lactoglobulin and lactoferrin (Vegarud et al., 2000). Calcite ($CaCO_3$) is another common form of Ca contained in dairy-based INF (Smith et al., 2013). Raman and FT-IR spectra can reveal information about the backbone and structure of sample molecules (Socrates, 2002). On the other hand, Ca element has a unique number of electrons, thus its atom will absorb or release energy in a pattern unique to its elemental identity. Consequently, atomic absorption or emission spectroscopy (i.e. AAS and LIBS) can detect Ca elements directly by its unique energy release pattern. It was observed in Supplementary (II) that for both Raman and FT-IR methods, the best performing models were developed using the

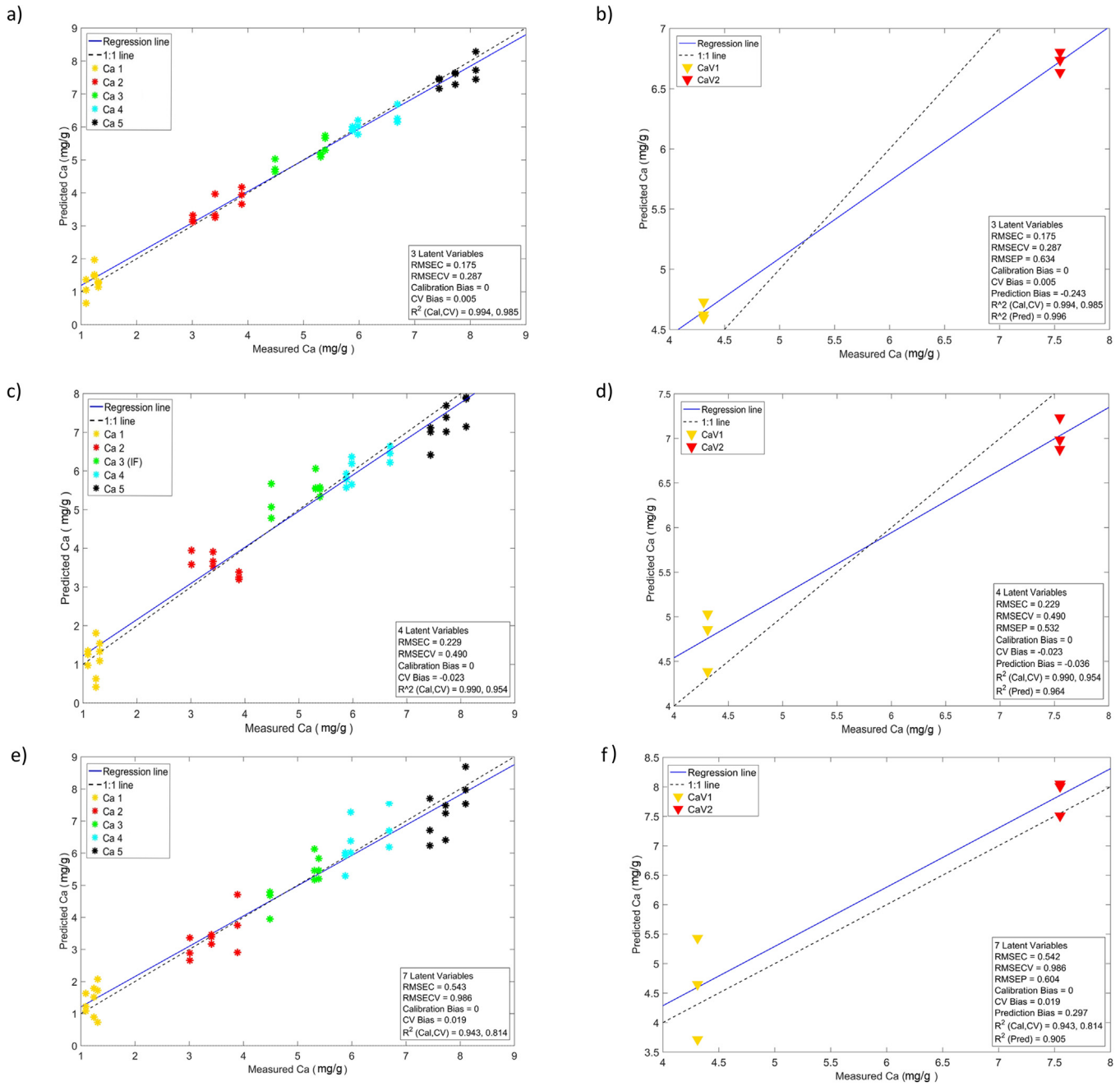

Fig. 3. PLS regression plots of INF samples on measured Ca (X-axis) vs. predicted Ca (Y-axis) of the best performed model: a) cross-validation and b) prediction based on LIBS spectra; c) cross-validation and d) prediction based on Raman spectra; e) cross-validation and f) prediction based on FT-IR spectra.

wavelength range of 450–2800 cm^{-1}. This wavelength range include almost all the chemical bonds that related to milk proteins, peptides and calcite. The results also show that the models developed based on FT-IR spectra are less robust than those developed on LIBS and Raman spectra; this was manifested mainly by the facts that the PLSR modelling using FT-IR spectral data relied on more latent variables (PLS loadings) and yielded lower R^2 values, higher absolute bias values and RMSE values. However, the models developed on the data fusion of Raman and FT-IR spectral features (i.e. the LV scores) are more robust than the models developed using individual FT-IR or Raman spectral features. On the other hand, the developed models based on the mid-level fusion of the LV scores (Fig. 1–Data fusion (II)) demonstrated better prediction performances than the models developed using the lower level data fusion of spectral variables (Fig. 1 – Data fusion (I) A& B).

The prediction potential of the models was also evaluated by the LOD values. The highest LOD value was obtained for FT-IR method and was 3.963 mg/g. LODs that derived from the best models based on LIBS and Raman spectra were 1.079 mg/g and 1.872 mg/g, respectively. The LOD values for the models developed using Data fusion-(II) was 2.036 mg/g and for that developed using Data fusion-(I) (Fig. 1) was 2.714 mg/g. As the LOD values represent the lowest quantity of a substance that can be distinguished by the developed models from the absence of this substance (with 99% of confidence) (MacDougall & Crummett, 1980); the models developed using the spectral data of LIBS demonstrated the best performance to detect the lowest quantity of Ca content in INF. Nevertheless, the model developed using VIP selected Raman spectral variables (n = 638) obtained the overall second-best performance for the detection of the lowest quantity of Ca in INF.

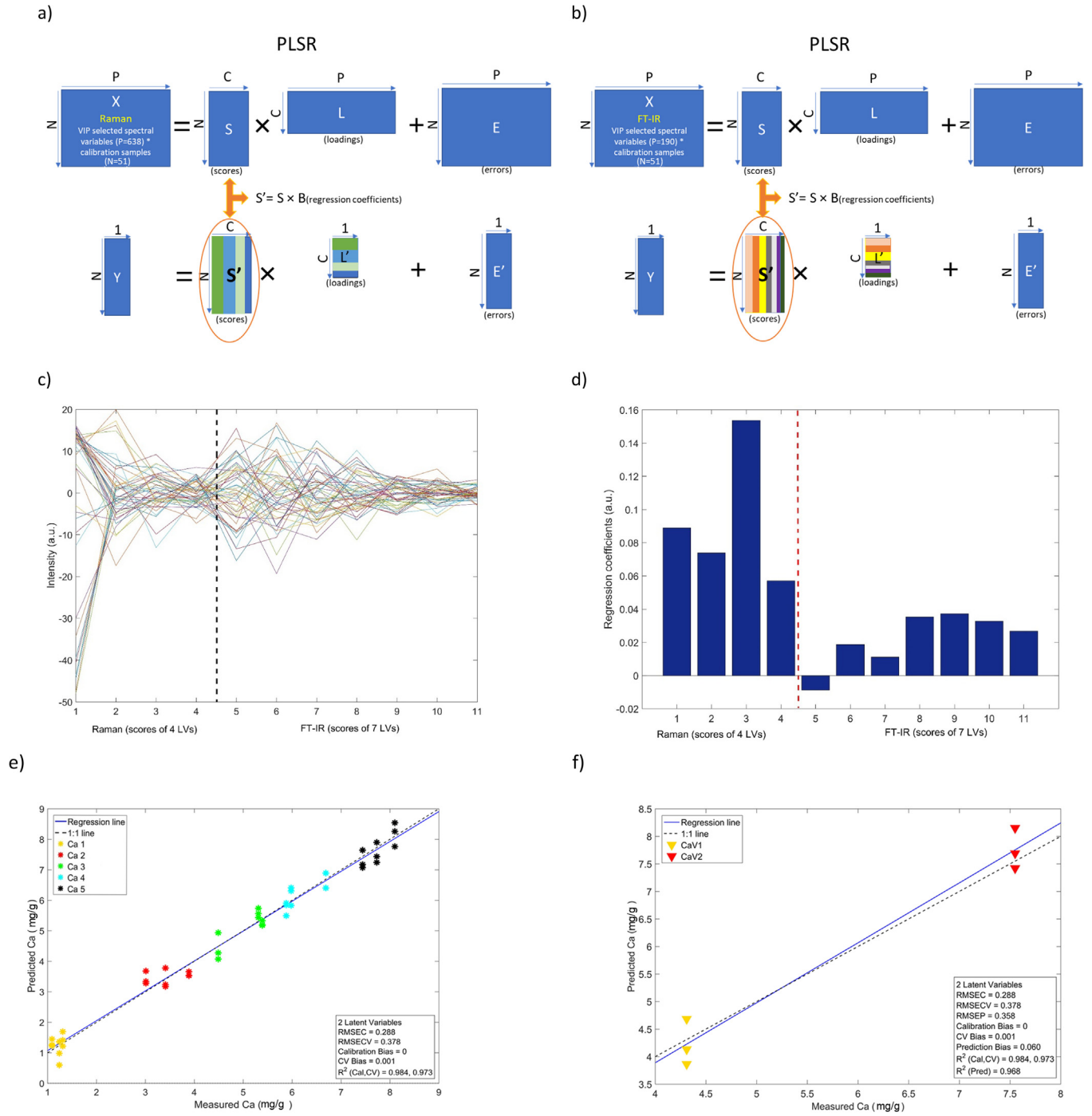

Fig. 4. Results of Data fusion (II): the procedures to extract PLS scores from PLS modelling based on a) Raman spectra, b) FT-IR spectra; c) the plot of PLS score concatenation; d) the regression coefficient plot of PLSR modelling based on fused scores; PLS regression plots of INF samples on measured Ca (X-axis) vs. predicted Ca (Y-axis): e) cross-validation and f) prediction.

3.5. Discussion of regression coefficient intensities for Ca prediction

In order to find the direct evidence of the spectral information related to Ca content, regression coefficient intensities of all LIBS spectral variables (181.418–904.192 nm), individual Raman and FT-IR spectral variables in the selected wavelength range (450–2800 cm^{-1}) were calculated during PLSR modelling.

In Fig. 5a, high regression coefficient intensities with positive values were shown mostly at the Ca related wavelengths and rarely at N, K and O related wavelengths. Other relatively high intensities with negative values are shown at C, Mg, CN, Na, H and Mg emission related wavelengths. This result was derived from the PLSR modelling for Ca prediction using four latent variables and it indicates that Ca emission lines positively influence the regression model for Ca prediction while emission lines of other elements may negatively influence the prediction or cause errors.

Fig. 5b shows that an outstanding high-intensity peak exists at 1085 cm^{-1} of Raman shifts, which has been approved to have a great amount of influence to quantify calcite ($CaCO_3$) in INF powder (Smith et al., 2013). In the current study, the preparation of samples at different Ca content levels was controlled by the estimation on Ca content that provided by the manufacture. In Fig. 5c, positively high regression

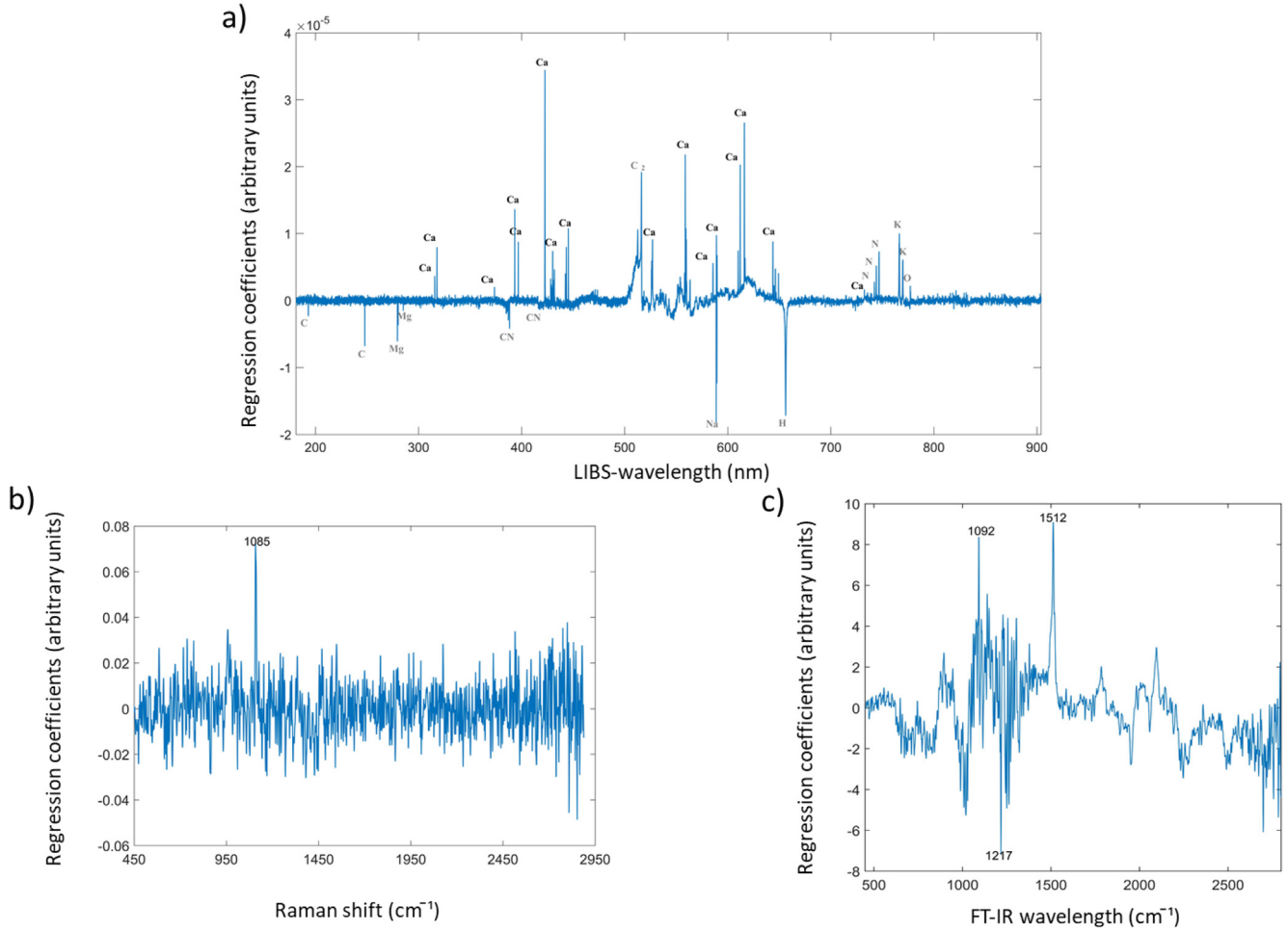

Fig. 5. Regression coefficients plots of PLSR models developed using a) LIB spectral variables (185–904 nm); b) Raman spectral variables (450–2800 cm^{-1}); c) FT-IR spectral variables (450–2800 cm^{-1}).

coefficient intensities of the FT-IR spectral wavelengths are shown at 1019, 1028 and 1517 cm^{-1} in the wavelength ranges of 1000–1120 cm^{-1} and 1450–1530 cm^{-1}, which are assigned to CO_3^{2-} and PO_4^{3-} of $CaCO_3$ and the compound (Ca-PO_4 = Ca = PO_4-Ca) bound to casein, respectively (Berzina-Cimdina & Borodajenko, 2012). As calcite ($CaCO_3$) was the only controlled source of Ca to modify the Ca content of samples prepared in this study, the difference of calcite content in samples could have been tracked using Raman or FT-IR spectral features. To the same effect, other Ca source in INF could have also been determined without tracking. Therefore, the regression coefficients of calcite related Raman or FT-IR wavelengths can be used to inspect the potential of vibrational spectroscopy for the determination of the anions or backbones of Ca ions bonded chemical functional groups in INF. Both Raman and FT-IR spectra contain multivariate information on the functional groups that Ca is bounded to; therefore, their correlated Ca ions can be determined using the combination of vibrational spectroscopy (i.e. Raman and FT-IR) and multivariate analysis.

4. Conclusion

In this study, both atomic spectroscopy (i.e. AAS and LIBS) and vibrational spectroscopy (i.e. Raman and FT-IR) were employed to quantify Ca content in INF. AAS and LIBS are originally designed to destruct complex INF materials in order to isolate various elements including calcium. AAS was used as a reference method to quantify Ca content in the samples; LIBS combined with PLSR modelling was used to develop a rapid method for Ca prediction and to compare with the prediction results of PLSR modelling based on Raman and FT-IR spectral information. Overall, the model developed using LIBS achieved the best prediction performance (R^2CV-0.985, RMSECV-0.287 mg/g; R^2P-0.996, RMSEP-0.634 mg/g; LOD-1.079 mg/g). The second best-performed model was developed using the mid-level data fusion of both Raman and FT-IR spectral features (R^2CV-0.973, RMSECV- 0.378 mg/g; R^2P-0.968, RMSEP-0.358 mg/g; LOD-2.036 mg/g). Based on the model performances, it also can be concluded that Raman spectroscopy is more effective than FT-IR spectroscopy to determine the Ca bounded functional groups and protein backbones in INF. Chemometric approaches including algorithms of baseline correction, variable selection, regression modelling and data fusions, allowed to isolate and interpret the informative spectral features related to Ca content and eventually to develop models for the quantification purpose. Results demonstrated the feasibilities of Raman and FT-IR combined with chemometrics to quantify Ca content in INF. The results obtained in this study also confirmed that LIBS combined with chemometrics can be a rapid and low-cost method for calcium quantification and should be considered as a PAT strategy in the dairy industry.

CRediT authorship contribution statement

Ming Zhao: Conceptualization, Methodology, Software, Formal analysis, Investigation, Data curation, Writing - original draft. **Maria Markiewicz-Keszycka:** Conceptualization, Methodology, Formal analysis, Investigation, Data curation, Writing - original draft. **Renwick J.**

Beattie: Methodology, Software. **Maria P. Casado-Gavalda:** Methodology, Investigation, Software. **Xavier Cama-Moncunill:** Methodology, Data curation. **Colm P. O'Donnell:** Writing - review & editing, Supervision. **Patrick J. Cullen:** Writing - review & editing, Resources, Project administration. **Carl Sullivan:** Methodology, Writing - review & editing, Resources, Supervision.

Declaration of Competing Interest

The authors declare that they have no known competing financial interests or personal relationships that could have appeared to influence the work reported in this paper.

Acknowledgements

The authors would like to acknowledge funding from the Food Institutional Research Measure, administered by the Department of Agriculture, Food and the Marine, Ireland (Grant agreement: 14/F/866).

Appendix A. Supplementary data

Supplementary data to this article can be found online at https://doi.org/10.1016/j.foodchem.2020.126639.

References

Ahmad, S., & Guo, M. (2014). Infant formula quality control. *Human milk biochemistry and infant formula manufacturing technology* (pp. 246–272). Elsevier. https://doi.org/10.1533/9780857099150.3.246.

Allegrini, F., & Olivieri, A. C. (2014). IUPAC-consistent approach to the limit of detection in partial least-squares calibration. *Analytical Chemistry, 86*(15), 7858–7866. https://doi.org/10.1021/ac501786u.

Almeida, M. R., Oliveira, K.de S., Stephani, R., & de Oliveira, L. F. C. (2011). Fourier-transform Raman analysis of milk powder: A potential method for rapid quality screening. *Journal of Raman Spectroscopy, 42*(7), 1548–1552. https://doi.org/10.1002/jrs.2893.

Arifin, M., Swedlund, P. J., Hemar, Y., & McKinnon, I. R. (2014). Calcium phosphates in Ca2 + -fortified milk: Phase identification and quantification by Raman spectroscopy. *Journal of Agricultural and Food Chemistry, 62*(50), 12223–12228. https://doi.org/10.1021/jf503602n.

Beattie, R. J., Bell, S. J., Farmer, L. J., Moss, B. W., & Patterson, D. (2004). Preliminary investigation of the application of Raman spectroscopy to the prediction of the sensory quality of beef silverside. *Meat Science, 66*(4), 903–913. https://doi.org/10.1016/j.meatsci.2003.08.012.

Berzina-Cimdina, L., & Borodajenko, N. (2012). Research of calcium phosphates using Fourier Transform Infrared Spectroscopy. p. Ch. 6 In N. B. E.-T. Theophanides (Ed.). *Infrared Spectroscopy - Materials Science, Engineering and Technology*Rijeka: IntechOpen. https://doi.org/10.5772/36942.

Bonfatti, V., Degano, L., Menegoz, A., & Carnier, P. (2016). Short communication: Mid-infrared spectroscopy prediction of fine milk composition and technological properties in Italian Simmental. *Journal of Dairy Science, 99*(10), 8216–8221. https://doi.org/10.3168/jds.2016-10953.

Bunaciu, A. A., & Aboul-Enein, H. Y. (2017). Vibrational Spectroscopy Applications in Drugs Analysis. In Lindon, J. C., Tranter, G. E., & D. W. B. T.-E. of S. and S. (Third E. Koppenaal (Eds.). Oxford: Academic Press. DOI: 10.1016/B978-0-12-409547-2.12214-0 pp. 575–581.

Cama-Moncunill, X., Markiewicz-Keszycka, M., Dixit, Y., Cama-Moncunill, R., Casado-Gavalda, M. P., Cullen, P. J., et al. (2017). Feasibility of Laser-Induced Breakdown Spectroscopy (LIBS) as an at-line validation tool for calcium determination in infant formula. *Food Control, 78*, 304–310. https://doi.org/10.1016/j.foodcont.2017.03.005.

Chong, I.-G., & Jun, C.-H. (2005). Performance of some variable selection methods when multicollinearity is present. *Chemometrics and Intelligent Laboratory Systems, 78*, 103–112. https://doi.org/10.1016/j.chemolab.2004.12.011.

Chou, I.-M., & Wang, A. (2017). Application of laser Raman micro-analyses to Earth and planetary materials. *Journal of Asian Earth Sciences, 145*, 309–333. https://doi.org/10.1016/j.jseaes.2017.06.032.

Chukanov, N. V. (2014). *The application of IR Spectroscopy to the Investigation of Minerals BT - Infrared spectra of mineral species: Extended library*. Dordrecht: Springer Netherlands1–19. https://doi.org/10.1007/978-94-007-7128-4_1.

Cullen, P. J., O'Donnell, C. P., & Fagan, C. C. (2014). Benefits and challenges of adopting PAT for the food industry. In C. P. O'Donnell, C. Fagan, & P. J. Cullen (Eds.). *Process Analytical Technology for the Food Industry* (pp. 1–5). New York, NY: Springer New York. https://doi.org/10.1007/978-1-4939-0311-5_1.

El-abassy, R., Eravuchira, P., Donfack, P., von der Kammer, B., & Materny, A. (2011). Fast determination of milk fat content using Raman spectroscopy. *Vibrational Spectroscopy - VIB SPECTROSC, 56*. https://doi.org/10.1016/j.vibspec.2010.07.001.

Fleet, M. E. (2017). Infrared spectra of carbonate apatites: Evidence for a connection between bone mineral and body fluids. *American Mineralogist, 102*(1), 149–157. https://doi.org/10.2138/am-2017-5704.

Harding, J. E., Cormack, B. E., Alexander, T., Alsweiler, J. M., & Bloomfield, F. H. (2017). Advances in nutrition of the newborn infant. *The Lancet, 389*(10079), 1660–1668. https://doi.org/10.1016/S0140-6736(17)30552-4.

Juanéda, P., Ledoux, M., & Sébédio, J.-L. (2007). Analytical methods for determination oftrans fatty acid content in food. *European Journal of Lipid Science and Technology, 109*(9), 901–917. https://doi.org/10.1002/ejlt.200600277.

Kirk, J., Dann, S., Blatchford, G., & C. (2007). Lactose: A definitive guide to polymorph determination. *International Journal of Pharmaceutics, 334*. https://doi.org/10.1016/j.ijpharm.2006.10.026.

Kramida, A., Ralchenko, Y., Reader, J., & team, N. A. (2016). NIST atomic spectra database (version 5.4). Retrieved July 17, 2018, from https://www.nist.gov/pml/atomic-spectra-database.

Lei, Y., Zhou, Q., Zhang, Y., Chen, J., Sun, S., & Noda, I. (2010). Analysis of crystallized lactose in milk powder by Fourier-transform infrared spectroscopy combined with two-dimensional correlation infrared spectroscopy. *Journal of Molecular Structure, 974*(1), 88–93. https://doi.org/10.1016/j.molstruc.2009.12.030.

Li-Chan, E. C. Y. (1996). The applications of Raman spectroscopy in food science. *Trends in Food Science & Technology, 7*(11), 361–370. https://doi.org/10.1016/S0924-2244(96)10037-6.

Liu, Y., Eriksson, M., Jin, Z., Nygren, M., & Shen, Z. (2014). Micro-hydrothermal reactions mediated grain growth during spark plasma sintering of a carbonate-containing hydroxyapatite nanopowder. *Journal of the European Ceramic Society, 34*(16), 4395–4401. https://doi.org/10.1016/j.jeurceramsoc.2014.06.026.

MacDougall, D., Crummett, W. B., et al. (1980). Guidelines for data acquisition and data quality evaluation in environmental chemistry. *Analytical Chemistry, 52*(14), 2242–2249. https://doi.org/10.1021/ac50064a004.

Markiewicz-Keszycka, M., Casado-Gavalda, M. P., Cama-Moncunill, X., Cama-Moncunill, R., Dixit, Y., Cullen, P. J., et al. (2018). Laser-induced breakdown spectroscopy (LIBS) for rapid analysis of ash, potassium and magnesium in gluten free flours. *Food Chemistry, 244*, 324–330. https://doi.org/10.1016/j.foodchem.2017.10.063.

Rodrigues Júnior, P. H., de Sá Oliveira, K., de Almeida, C. E. R., De Oliveira, L. F. C., Stephani, R., da Pinto, M., et al. (2016). FT-Raman and chemometric tools for rapid determination of quality parameters in milk powder: Classification of samples for the presence of lactose and fraud detection by addition of maltodextrin. *Food Chemistry, 196*, 584–588. https://doi.org/10.1016/j.foodchem.2015.09.055.

Rollins, N. C., Bhandari, N., Hajeebhoy, N., Horton, S., Lutter, C. K., Martines, J. C., et al. (2016). Why invest, and what it will take to improve breastfeeding practices? *The Lancet, 387*(10017), 491–504. https://doi.org/10.1016/S0140-6736(15)01044-2.

Safar, M., Bertrand, D., Robert, P., Devaux, M. F., & Genot, C. (1994). Characterization of edible oils, butters and margarines by Fourier transform infrared spectroscopy with attenuated total reflectance. Journal of the American Oil Chemists' Society, 71(4), 371–377. DOI: 10.1007/BF02540516.

Smith, G. P. S., Gordon, K. C., & Holroyd, S. E. (2013). Raman spectroscopic quantification of calcium carbonate in spiked milk powder samples. *Vibrational Spectroscopy, 67*, 87–91. https://doi.org/10.1016/j.vibspec.2013.04.005.

Socrates, G. (2002). Infrared and Raman Characteristic Group Frequencies: Tables and Charts. 3rd ed By George Socrates (The University of West London, Middlesex, U.K.). J. Wiley and Sons: Chichester. 2001. xviii + 348 pp. $185.00. ISBN: 0-471-85298-8. Journal of the American Chemical Society, 124(8), 1830–1830. DOI: 10.1021/ja0153520.

Strain, J. J. & Cashman, K. D. (2002). Minerals and trace elements. In & F. J. K. M. J. Gibney, H. H. Vorster (Ed.), Introduction to Human Nutrition (pp. 178–185). Berlin: Blackwell Sciences Press.

The European communities. (2006). COMMISSION DIRECTIVE 2006/141/EC of 22 December 2006 on infant formulae and follow-on formulae and amending Directive 1999/21/EC. Retrieved July 16, 2018, from https://eur-lex.europa.eu/legal-content/EN/ALL/?uri = CELEX%3A32006L0141.

Vegarud, G. E., Langsrud, T., & Svenning, C. (2000). Mineral-binding milk proteins and peptides; occurrence, biochemical and technological characteristics. British Journal of Nutrition, 84(S1), 91–98. DOI: 10.1017/S0007114500002300.

Victora, C. G., Bahl, R., Barros, A. J. D., França, G. V. A., Horton, S., Krasevec, J., et al. (2016). Breastfeeding in the 21st century: Epidemiology, mechanisms, and lifelong effect. *The Lancet, 387*(10017), 475–490. https://doi.org/10.1016/S0140-6736(15)01024-7.

Visentin, G., Penasa, M., Gottardo, P., Cassandro, M., & De Marchi, M. (2016). Predictive ability of mid-infrared spectroscopy for major mineral composition and coagulation traits of bovine milk by using the uninformative variable selection algorithm. *Journal of Dairy Science, 99*(10), 8137–8145. https://doi.org/10.3168/jds.2016-11053.

Walsh, H. (2014). Infant formula analysis. *Human milk biochemistry and infant formula manufacturing technology* (pp. 311–344). Elsevier. https://doi.org/10.1533/9780857099150.3.311.

Wubshet, S. G., Wold, J. P., Böcker, U., Sanden, K. W., & Afseth, N. K. (2019). Raman spectroscopy for quantification of residual calcium and total ash in mechanically deboned chicken meat. *Food Control, 95*, 267–273. https://doi.org/10.1016/j.foodcont.2018.08.017.

Zhao, M., Beattie, R. J., Fearon, A. M., O'Donnell, C. P., & Downey, G. (2015). Prediction of naturally-occurring, industrially-induced and total trans fatty acids in butter, dairy spreads and Cheddar cheese using vibrational spectroscopy and multivariate data analysis. *International Dairy Journal, 51*, 41–51. https://doi.org/10.1016/j.idairyj.2015.07.011.